

Measurement of 7,8-dihydro-8-oxo-2'-deoxyguanosine metabolism in MCF-7 cells at low concentrations using accelerator mass spectrometry

Sang Soo Hah, Janna M. Mundt, Hyung M. Kim, Rhoda A. Sumbad, Kenneth W. Turteltaub, and Paul T. Henderson*

Chemistry, Materials, and Life Sciences Directorate and Center for Accelerator Mass Spectrometry, Lawrence Livermore National Laboratory, 7000 East Avenue, L-452, Livermore, CA 94551

Edited by Philip C. Hanawalt, Stanford University, Stanford, CA, and approved May 24, 2007 (received for review February 24, 2007)

Growing evidence suggests that oxidative damage to cells generates mutagenic 7,8-dihydro-8-oxo-2'-deoxyguanosine (8-oxodG), which may initiate diseases related to aging and carcinogenesis. Kinetic measurement of 8-oxodG metabolism and repair in cells has been hampered by poor assay sensitivity and by difficulty characterizing the flux of oxidized nucleotides through the relevant metabolic pathways. We report here the development of a sensitive and quantitative approach to characterizing the kinetics and metabolic sources of 8-oxodG in MCF-7 human breast cancer cells by accelerator mass spectrometry. We observed that [¹⁴C]8-oxodG at medium concentrations of up to 2 pmol/ml was taken up by MCF-7 cells, phosphorylated to mono-, di-, and triphosphate derivatives, and incorporated into DNA. Oxidative stress caused by exposure of the cells to 17 β -estradiol resulted in a reduction in the rate of [¹⁴C]8-oxodG incorporation into DNA and an increase in the ratio of 8-oxodG monophosphate (8-oxodGMP) to 8-oxodG triphosphate (8-oxodGTP) in the nucleotide pool. 17 β -Estradiol-induced oxidative stress up-regulated the nucleotide pool cleansing enzyme MTH1 and possibly other Nudix-related pyrophosphohydrolases. These data support the conclusion that 8-oxodGTP is formed in the nucleotide pool by both 8-oxodG metabolism and endogenous reactive oxygen species. The metabolism of 8-oxodG to 8-oxodGTP, followed by incorporation into DNA is a mechanism by which the cellular presence of this oxidized nucleoside can lead to mutations.

DNA repair | nucleoside metabolism | oxidative stress | breast cancer

One of the most prevalent lesions found in DNA is 7,8-dihydro-8-oxo-2'-deoxyguanosine (8-oxodG) (Fig. 1A). If not repaired, it can direct incorporation of dATP by DNA polymerases, resulting in G \rightarrow T transversion mutations (1–4). Likewise, 8-oxodG triphosphate (8-oxodGTP) is a mutagenic substrate for DNA synthesis because it can be incorporated opposite adenine and cytosine resulting in A \rightarrow C and G \rightarrow T transversions (5–7).

To avoid mutations caused by 8-oxodG, *Escherichia coli* has evolved at least three enzymes that play pivotal roles in DNA repair (1–3). The DNA glycosylase formamidopyrimidine-DNA glycosylase (Fpg), also known as MutM, removes the oxidized base from 8-oxodG:dC base pairs. The MutY DNA glycosylase excises adenine misincorporated opposite 8-oxodG. MutM and MutY initiate downstream events that constitute the base excision repair (BER) pathway. In the nucleotide pool, the pyrophosphohydrolase MutT hydrolyzes 8-oxodGTP to 8-oxodG monophosphate (8-oxodGMP), reducing the concentration of 8-oxodGTP available for DNA synthesis. Mammals use repair enzymes that are functionally homologous to MutM, MutY, and MutT, including OGG1, MYH, and MutT homologous 1 (MTH1), respectively (3, 8).

Recently, 8-oxodG has been characterized as a chemically unstable intermediate because of a low oxidation potential compared with the parent dG (9, 10). The oxidation of 8-oxodG produces several 2'-deoxynucleosides, including derivatives of

cyanuric acid, oxaluric acid, oxazalone, and at least three hydantoin derivatives [for structures see supporting information (SI) Fig. 6] (10–13). These species are severalfold more mutagenic than 8-oxodG in DNA as measured with a bacteriophage-based assay (14–16). Although these 8-oxodG-derived products are likely to exist in cells, only the spiroiminodihydantoin derivative has been reported to form in *E. coli* (17). Some 8-oxodG oxidation products are recognized by purified BER enzymes such as MutM, OGG1, NIEL1, and NIEL2 (11, 18–20).

In contrast to DNA repair of 8-oxodG, little information on the metabolism of 8-oxodG to 8-oxodGTP is available. Currently, the prevailing paradigm is that 8-oxodGTP is predominantly formed directly from dGTP in cells and that there may be some contribution from 8-oxodG diphosphate (8-oxodGDP) after conversion to the triphosphate by nucleotide diphosphate kinase (3). There is no reported evidence that unphosphorylated 8-oxodG is a substrate for nucleotide salvage. The paucity of data concerning nucleotide salvage of oxidized nucleotides is the result of a lack of analytical approaches with the sensitivity, specificity, and ability to quantify metabolic fluxes at physiologically relevant concentrations of biochemicals in cells.

We have been developing the technique of accelerator mass spectrometry (AMS) as a possible solution to this issue of quantification of metabolic rates at cellular metabolite concentrations. We recently reported the synthesis of [¹⁴C]8-oxodG and preliminary measurement of its incorporation into the DNA of MCF-7 cells by using AMS (9). Thus, 8-oxodG metabolism is a useful model to test the utility of AMS for metabolic flux analysis. AMS is a well established technology for radiocarbon dating and is now used for tracing ¹⁴C-labeled compounds in biological systems (21). AMS affords subpicomole to zeptomole sensitivity in quantifying ¹⁴C-labeled metabolites with a few percent precision, depending on experimental conditions (21, 22). The method relies on measurement of ¹⁴C in a biological sample that has been converted to solid graphite before analysis, which facilitates high measurement sensitivity because of efficient ion current production in the AMS instrument. We report here the use of AMS in combination with other molecular biology tools to characterize the contribution of the nucleotide salvage pathway to 8-oxodG levels in genomic DNA and mea-

Author contributions: S.S.H. and J.M.M. contributed equally to this work; S.S.H., J.M.M., K.W.T., and P.T.H. designed research; S.S.H., J.M.M., H.M.K., and R.A.S. performed research; S.S.H., J.M.M., K.W.T., and P.T.H. analyzed data; and S.S.H. and P.T.H. wrote the paper.

The authors declare no conflict of interest.

This article is a PNAS Direct Submission.

Abbreviations: AMS, accelerator mass spectrometry; BER, base excision repair; dG, 2'-deoxyguanosine; E₂, 17 β -estradiol; Fpg, formamidopyrimidine-DNA glycosylase; MTH1, MutT homologous 1; 8-oxodG, 7,8-dihydro-8-oxo-2'-deoxyguanosine; 8-oxodGMP, 8-oxodG monophosphate; 8-oxodGDP, 8-oxodG diphosphate; 8-oxodGTP, 8-oxodG triphosphate; qRT-PCR, quantitative RT-PCR.

*To whom correspondence should be addressed. E-mail: henderson48@llnl.gov.

This article contains supporting information online at www.pnas.org/cgi/content/full/0701733104/DC1.

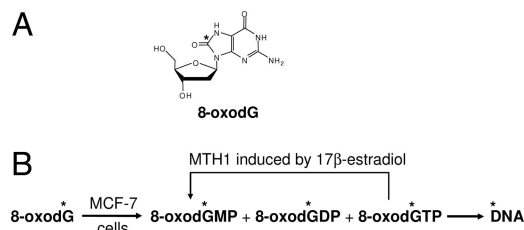


Fig. 1. Chemical structure and mechanistic pathway for 8-oxodG metabolism. (A) Chemical structure of [^{14}C]8-oxodG. (B) Schematic of 8-oxodG metabolism to nucleotide phosphate derivatives and putative mechanism of MTH1-mediated retardation of 8-oxodGTP incorporation into DNA. The asterisk represents ^{14}C .

surement of BER rates *in situ*, and we provide evidence of further oxidation of the nucleoside under conditions of oxidative stress (Fig. 1B).

Results and Discussion

8-OxodG Incorporation into DNA of MCF-7 Cells. We synthesized [^{14}C]8-oxodG (9) and measured its incorporation into the DNA of MCF-7 cells at a variety of concentrations (Fig. 2A). Dividing cells were dosed with [^{14}C]8-oxodG 2 days before confluence, and total genomic DNA was isolated by using conditions that prevented artifactual oxidation (SI Fig. 7). Incorporation of [^{14}C]8-oxodG into DNA ranged from ≈ 5 to 130 amol/ μg of DNA, demonstrating that 8-oxodG can be converted to a triphosphate derivative and incorporated into total genomic DNA. The maximum incorporation of radiocarbon into DNA corresponded to $\approx 2,000$ molecules per cell or ≈ 3 molecules per 10^7 normal nucleotides, which approached background 8-oxodG levels in the DNA of many cell types (23, 24). The high levels of 8-oxodG incorporation into DNA observed may have resulted from altered DNA repair pathways. For example, it has been reported that the oxidized nucleoside triphosphate pool is a significant contributor to genomic instability in mismatched repair-deficient cells (25, 26). However, this situation is unlikely for MCF-7 cells because there are reports of mismatch repair proficiency for these cells (27–29).

At the 600 dpm [^{14}C]8-oxodG dose, an asymptote was nearly reached that may represent saturation of the nucleotide salvage pathway. Alternatively, this concentration may be the point at which 8-oxodG becomes toxic. However, no increased cell death occurred with 8-oxodG exposure (SI Fig. 8). The 300 dpm [^{14}C]8-oxodG dose, which represents a not-quite-saturating dose, was used for subsequent experiments.

To better understand the uptake and fate of the [^{14}C]8-oxodG in the cells, we measured the distribution of the compound in various components of the cell culture system including the medium, cells, and purified DNA (Fig. 2B). Cells were incubated in the presence of 300 dpm (10.8 pmol total dose of 8-oxodG) of [^{14}C]8-oxodG for 4 days. AMS samples were prepared in triplicate from 20- μl aliquots each of the medium, lysed cells, and purified DNA. The AMS data allowed calculation of the fractional amount of ^{14}C in each sample. Of the total radiocarbon, $92.0 \pm 1.2\%$ persisted in the medium. The remaining radiocarbon was localized on or inside the cells, with $1.6 \pm 0.1\%$ uptake of ^{14}C into nuclear DNA. This amount of radiocarbon in the DNA would be difficult to characterize by standard scintillation counting (a few disintegrations per minute) or other types of mass spectrometry, but it was easily quantifiable by AMS. The mass distribution data indicate that a substantial amount of the exogenous [^{14}C]8-oxodG was taken into the cells and incorporated into the DNA.

The kinetics of incorporation and DNA repair of [^{14}C]8-oxodG were compared with a [^{14}C]dG control. Fig. 2C shows the

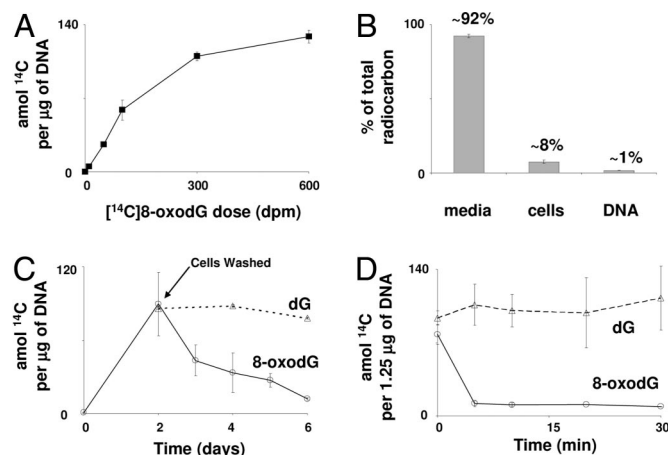


Fig. 2. Characterization of 8-oxodG incorporation into DNA of MCF-7 cells via nucleotide salvage. (A) ^{14}C content in DNA (amol/ μg) extracted from cells after 2 days of growth with increasing concentrations of [^{14}C]8-oxodG. The highest dose of 600 dpm contained 21.6 pmol of compound with a specific activity of 11 mCi/mmol (1 Ci = 37 GBq; 20% of the molecules contain a ^{14}C atom). (B) Mass distribution in growth medium, in MCF-7 cells, and in extracted DNA, respectively, after a 4-day incubation of MCF-7 cells with 300 dpm of [^{14}C]8-oxodG. (C) DNA repair in cells dosed for 2 days followed by washing and replenishment with ^{14}C -free medium for another 0, 1, 2, 3, and 4 days (circles represent [^{14}C]8-oxodG dosing, and triangles represent [^{14}C]dG dosing). (D) ^{14}C concentration (amol/1.25 μg) in extracted DNA from cells dosed with 300 dpm of [^{14}C]8-oxodG for 2 days after Fpg digestion. [^{14}C]8-oxodG (circles) was rapidly excised from the duplex DNA compared with [^{14}C]dG (triangles).

kinetics of radiocarbon incorporation and removal from DNA in cells dosed with either [^{14}C]8-oxodG or [^{14}C]dG. Cells were then washed repeatedly with PBS followed by replenishment with ^{14}C -free medium to measure the rate of DNA repair over several days. We anticipated degradation of the damaged nucleotide into DNA compared with dG (3–6). Unexpectedly, the rate of incorporation into DNA of [^{14}C]8-oxodG was approximately equal to that of [^{14}C]dG after 2 days, indicating little or no discrimination against 8-oxodG during nucleotide salvage under the growth conditions used.

Four days after replenishment with ^{14}C -free medium, nearly all of the [^{14}C]8-oxodG was removed from the cellular DNA, presumably by BER ($t_{1/2} \approx 2$ days), whereas no loss of [^{14}C]dG was observed under identical experimental conditions (Fig. 2C). The observed steady-state concentration for [^{14}C]dG is presumably caused by reduced proliferation upon confluence, which was reached 2 days after dosing with the radiocarbon-labeled nucleosides.

Although [^{14}C]8-oxodG was incorporated into the DNA, the radiocarbon-containing nucleotides may have been in altered form or noncovalently bound to the DNA. To address these concerns, we incubated nuclear DNA from the cells with Fpg, the glycosylase and apurinic-lyase responsible for excising several oxidized purines during BER in *E. coli*. (Fig. 2D). Excision of ^{14}C -containing base damage was rapid ($t_{1/2} \approx 5$ min) in the DNA from the cells grown with [^{14}C]8-oxodG (Fig. 2D, circles), whereas the [^{14}C]dG-dosed control was completely resistant to the DNA glycosylase (Fig. 2D, triangles). Because Fpg is specific for the excision of oxidized purines in duplex DNA, this experiment supports the conclusion that [^{14}C]8-oxodGTP and [^{14}C]dGTP were produced from the respective ^{14}C -labeled nucleosides and incorporated into DNA.

Because Fpg has numerous oxidized purine substrates, the excised product(s) may not have been 8-oxodG, but rather other

Clearly, [^{14}C]8-oxodG incorporation into DNA is slowed in an E_2 concentration-dependent manner, although these estrogen receptor-positive cells proliferate in response to E_2 exposure (SI Fig. 9). For example, the rate of incorporation of 8-oxodG into DNA was reduced ≈ 3 -fold at a concentration of 10 nM E_2 after 2 days of growth, with an even greater effect with 100 nM E_2 . We interpret the decrease in radiocarbon incorporation into DNA as a result of increased guanine nucleotide and nucleoside oxidation products competing with [^{14}C]8-oxodG incorporation into DNA.

To determine whether the reduction of radiocarbon incorporation efficiency was specific to 8-oxodG, we performed control experiments in which MCF-7 cells were dosed with [^{14}C]dG in the presence or absence of 100 nM E_2 . As was the case with [^{14}C]8-oxodG, E_2 caused a lower concentration of radiocarbon to be incorporated into the DNA (SI Fig. 10). This observation may be the result of the involvement of MTH1 because both 8-oxodGTP and dGTP are substrates for this enzyme (4, 33). Although dGTP is a poorer substrate, there is likely to be a million-fold or greater excess of dGTP in the cells compared with 8-oxodGTP. Because the guanine nucleobase in DNA is not a substrate for the canonical BER enzymes such as MYH and OGG1, these data indicate that the modulation of the radiocarbon-labeled purines in the DNA is predominantly controlled in the nucleotide pool.

Samples from day 4 after dosing with E_2 were digested and measured by HPLC-AMS for 8-oxodG modification caused by oxidative stress (Fig. 4B). In the absence of E_2 , the major peak coeluted with authentic 8-oxodG and corresponded to ≈ 8 fmol of [^{14}C]8-oxodG. A minor peak that eluted ≈ 1 min before the 8-oxodG standard corresponded to ≈ 100 amol of product, assuming no change in specific activity and a single species in the peak. The identity of this minor peak is unknown because there is too little material for other types of analysis and no standards for retention time comparison. In contrast, the chromatogram derived from E_2 -exposed MCF-7 cells yielded a drastically different product distribution. In the cells dosed with 100 nM E_2 , an ≈ 2 -fold higher concentration of the earlier eluting product was formed (≈ 200 amol/fraction), and at least five additional peaks were formed at levels ranging from 50–100 amol per fraction. The identification of these products will be investigated in future work. Clearly, E_2 modifies the radiocarbon-labeled nucleoside, either in the cytoplasm or in the DNA, to form derivatives that may be 8-oxodG oxidation products.

To assess the role of MTH1 in the E_2 -mediated 8-oxodG incorporation into DNA, we examined MTH1 expression with Western blotting and quantitative RT-PCR (qRT-PCR) (Fig. 4C). Increasing concentrations of E_2 caused an overall several-fold increase in MTH1 protein and mRNA compared with undosed control. Addition of unlabeled 8-oxodG had no effect on MTH1 protein levels in the cells (SI Fig. 11). These data imply that E_2 induces MTH1, thus partially retarding 8-oxodG incorporation into DNA.

Although we can neither verify nor rule out that this specific protein is solely responsible for the modulation of 8-oxodG incorporation into DNA in these cells, our data collectively demonstrate that MTH1 or other Nudix-related pyrophosphohydrolases act to reduce the incorporation of the increasing concentrations of oxidized nucleotides into DNA under conditions of oxidative stress caused by E_2 . This conclusion is supported by recent studies reporting that MTH1 expression levels increase with oxidative stress caused by ionizing radiation and hydrogen peroxide (34, 35). This phenomenon may be related to the observed increase in MTH1 concentration by as much as 10-fold in a variety of cancerous tissues compared with surrounding normal tissues (3, 36–39).

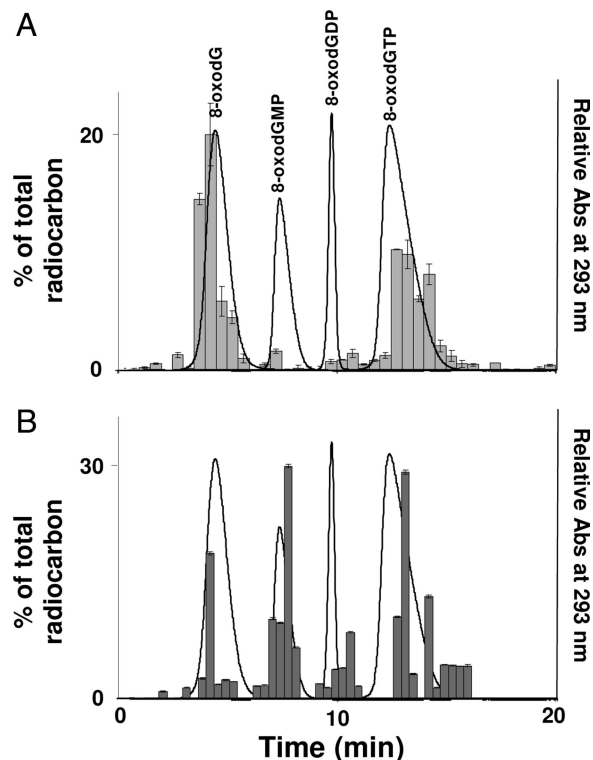


Fig. 5. Anion exchange chromatography analysis of 8-oxodG phosphorylation in MCF-7 cells dosed with [^{14}C]8-oxodG. (A) Chromatogram of filtered cell extract from cells grown in the absence of E_2 . (B) Chromatogram of filtered cell extract from cells grown in the presence of 100 nM E_2 . The elution times of the radiocarbon-labeled fractions were compared with authentic standards of 8-oxodG, 8-oxodGMP, 8-oxodGDP, and 8-oxodGTP.

Metabolism of 8-OxodG to Nucleotide Phosphate Derivatives. To characterize the formation of 8-oxodG metabolism products in the nucleotide pool, we performed anion exchange HPLC-AMS on cytoplasmic extracts from cells grown in the absence or presence of 100 nM E_2 (Fig. 5). Fractions containing elevated radiocarbon coeluted with each of the standards of 8-oxodG, 8-oxodGMP, 8-oxodGDP, and 8-oxodGTP. Although there may be other species in the HPLC fractions, the data indicate that the [^{14}C]8-oxodG was converted to the respective mono-, di-, and triphosphates. Without supplemental E_2 , the predominant radiocarbon-labeled metabolite coeluted with authentic 8-oxodGTP. In the presence of 100 nM E_2 , the radiocarbon substantially increased in the fractions that coeluted with 8-oxodGMP and 8-oxodGDP compared with the 8-oxodGTP fraction, which is consistent with increased expression of MTH1 (Fig. 4C).

Because these experiments simply show coelution of 8-oxodG metabolites with authentic standards, this result alone does not prove the conversion of 8-oxodG to 8-oxodGMP, 8-oxodGDP, and 8-oxodGTP. However, the HPLC-AMS data combined with the observation that exogenous [^{14}C]8-oxodG is incorporated into DNA strongly support the interpretation that 8-oxodG is converted to a nucleotide triphosphate before incorporation into DNA.

Irregular expression of some DNA polymerases, such as pol β or pol η , may account for the observed efficient incorporation (40, 41). Although 8-oxodGTP is a poor substrate for most replicative DNA polymerases (42), it is important to consider that our results were obtained in a cellular environment that likely has cofactors or even unknown polymerases that allow efficient incorporation of 8-oxodGTP. This interpretation is

consistent with a recent report that exogenous 8-oxodGTP introduced into mammalian cells was incorporated into DNA and caused mutations (43). Characterization of DNA polymerase expression in MCF-7 cells or other cell lines may be helpful to validate our findings.

Although peaks corresponding to the mono-, di-, and triphosphates are present in both of the chromatograms, we have no direct evidence that 8-oxodG is phosphorylated in a stepwise fashion. A possible alternative may be metabolism of 8-oxodG by enzymes such as purine nucleoside phosphorylase, hypoxanthine-guanine phosphoribosyltransferase, and ribonucleotide reductase to produce 8-oxodGTP, as is the case with dG (44). The latter mechanism in conjunction with MTH1 would produce all of the observed intermediates and may be cell type-dependent. Future work will be performed to distinguish these two possible mechanisms.

The nucleoside incorporation and DNA repair data strongly suggest that 8-oxodG in the nucleotide pool is a substrate for phosphorylation and incorporation into DNA through nucleotide salvage as outlined in Fig. 1B. The efficient 8-oxodG incorporation relative to dG indicates that nucleotide salvage can be a source for 8-oxodG in genomic DNA. Accordingly, newly synthesized DNA may possess a significant fraction of the total 8-oxodG derived from the nucleotide pool. In the cells studied, the nucleotide salvage pathway appears rate-limiting and equal for dG and 8-oxodG incorporation into DNA. Clearly, the presence of 8-oxodG alone does not induce MTH1. Oxidative stress is required for induction or stabilization of MTH1. The actual contribution of nucleotide salvage to the endogenous concentration of 8-oxodG in DNA remains to be determined. However, it is tempting to speculate that rapidly dividing cells in a hyperoxidative environment, such as those involved in carcinogenesis with concomitant inflammation, will have a large degree of 8-oxodG incorporation by this pathway.

In summary, we demonstrated that exogenous 8-oxodG is converted to the triphosphate and incorporated into cellular DNA of MCF-7 cells from the nucleotide pool at levels that approach that of endogenous concentrations of the nucleobase. AMS is the only technology capable of sensitively and precisely measuring the kinetics of nucleoside incorporation into DNA at such low levels, potentially allowing observation of initiating events and characterization of pathways that are relevant to normal intermediary metabolism, carcinogenesis, or other diseases. Future work will focus on rigorous identification of the 8-oxodG metabolism and oxidation products in various cell lines and animal models and quantification of the flux of the relevant precursors through the pathways involved in nucleotide metabolism.

Materials and Methods

Cell Culture, Proliferation Assay, and Cell Death Assay. MCF-7 cells obtained from American Type Culture Collection (Manassas, VA), were maintained in DMEM/F-12 medium (Invitrogen, Carlsbad, CA) supplemented with 10% FBS/penicillin (50 units/ml)/streptomycin (50 μ g/ml). The cells were cultured at 37°C in a gas phase of air with 5% CO₂ and were dosed either with [¹⁴C]8-oxodG or [¹⁴C]dG 2 days before confluence. For the proliferation assay, cells were grown in carbon-stripped serum instead of FBS. Cells (50,000) were plated on day 0 and harvested each day by trypsin, and cells were counted by using a Coulter Counter. Cell death measurements were obtained with the trypan blue exclusion assay.

DNA Extraction from MCF-7 Cells. After incubation, the medium was removed, and the cells were washed three times with PBS. Cells were removed from the plate with trypsin, washed by centrifugation in PBS, and lysed with the detergent Nonidet P-40 to isolate the cell nuclei. DNA was purified from the lysis mixture by using a reverse-phase cartridge (Qiagen, Valencia, CA), after

RNase treatment. The spurious generation of 8-oxodG or its oxidation products during isolation of DNA was alleviated according to the literature (30, 45). AMS samples were prepared in triplicate from purified DNA (10 μ g) after addition of carrier carbon in the form of 1 μ l of tributyrin.

Fpg Digestion of Extracted DNA. A 10- μ l solution of 50 mM Tris-HCl, pH 7.5/2 mM EDTA/70 mM NaCl/1.25 μ g of extracted cellular DNA was mixed with 2 μ g of Fpg (Sigma, St. Louis, MO) in an equal volume of the same buffer (46). The reaction mixtures were incubated at 37°C for 0, 5, 10, 20, and 30 min, respectively. Reactions were terminated by heating at 70°C for 10 s followed by ethanol precipitation at -20°C. Each DNA pellet was dissolved in 1 ml of water, and the cleaved nucleotides were removed with an NAP-10 column (Amersham Biosciences, Piscataway, NJ) by gravity flow. Final DNA concentrations were measured by using UV absorbance at 260 nm followed by AMS analysis.

HPLC Separation After DNA Digestion. To the dried DNA sample, 13 μ l of 30 mM sodium acetate (pH 5.8), 10 μ l of 10 mM zinc chloride, and 4 units of nuclease P1 (1 unit/ μ l) were added, and the mixture was incubated at 37°C for 1 h. To the reaction mixture, 30 μ l of 30 mM sodium acetate (pH 7.4), 10 units of shrimp alkaline phosphatase (1 unit/ μ l), and 5 units of snake venom phosphodiesterase I (0.1 unit/ μ l) were added, and the mixture was incubated at 37°C for another hour. The reaction was stopped by centrifuging sample through an Ultrafree MC-membrane (Millipore, Billerica, MA) at 5,000 \times g for 60 min at 4°C, affording a mixture of nucleosides that were separated by HPLC by using a 250- \times 4.6-mm Hypersil ODS column (Thermo Electron Corporation, Waltham, MA). Solvents A and B were 50 mM ammonium formate (pH 6.7) and acetonitrile, respectively. An isocratic elution of 0% B for 5 min was followed by the gradient elution from 0% B to 7% B in 45 min. A flow rate of 1.0 ml/min was used, resulting in a retention time of \approx 32 min for 8-oxodG (Fig. 3; and for comparison with the retention times of dC, dG, dT, and dA under identical HPLC conditions, see SI Fig. 12). Products were monitored simultaneously at 254 nm, 230 nm, and 293 nm. Collected HPLC fractions were sampled for AMS analysis as described previously (30).

Western Blotting. Whole-cell extracts were harvested in SDS/sample buffer (40% glycerol/0.24 M Tris, pH 6.8/8% SDS/20% 2-mercaptoethanol), and protein concentrations were measured by the Bradford assay (Bio-Rad, Hercules, CA) in triplicate. The Nu-PAGE Western blotting system (Invitrogen) was used with 50 μ g of protein in a 4–12% 2-[bis-(2-hydroxyethyl)amino]-2-(hydroxymethyl)-1,3-propanediol (BisTris) Novex acrylamide Nu-PAGE gel according to the manufacturer's directions. Membranes were probed with α -MTH1 (Novus Biologicals, Littleton, CO), α -GAPDH (Abcam, Cambridge, MA), or α - α -tubulin clone TU-01 (Invitrogen). Secondary antibodies were α -mouse (Zymed Laboratories, South San Francisco, CA) or α -rabbit (Rockland, Gilbertsville, PA), both conjugated to horseradish peroxidase.

qRT-PCR Measurements. Primers against MTH1 and GAPDH were designed manually. Each primer was designed to span at least one intron to prevent amplification of any DNA carryover. The length of the amplified product was designed to be \approx 200 bp. Each primer set was assayed for high efficiency under the specified PCR conditions by using serial dilution of the template.

Once conditions were established, cells were harvested by using TRIzol reagent (Invitrogen) according to the manufacturer's protocols for RNA harvesting, with the inclusion of a shearing step with an 18-gauge needle after the initial addition

of TRIzol. RNA concentration was calculated by measuring sample absorbance at 260 nm.

Five micrograms of RNA was used to synthesize cDNA as directed by the manufacturer with SuperScript III reverse transcriptase (Invitrogen), dNTPs (Invitrogen), and random hexamer primers (Invitrogen).

Finally, a 1:10 dilution of the prepared cDNA was used as a template in combination with gene-specific primers and iQ SYBR Green supermix (Bio-Rad) for qRT-PCR. PCR was carried out at 95°C for 3 min followed by 40 cycles of 95°C for 15 s, then 58°C for 15 s, followed by 72°C for 30 s by using a SmartCycler (Cepheid, Sunnyvale, CA). The FAM Ct calculated by the Cepheid SmartCycler version 1.2 software was then analyzed manually for the difference between MTH1 and GAPDH (dCt). The difference was normalized to the wild-type control for the given experiment (ddCt). The final calculation of 2^{-ddCt} takes into account the exponential nature of PCR and was compared across cell lines to determine the level of transcript under given conditions as seen in the figures. The S.E. is reported based on the average of three experiments.

Anion Exchange HPLC Separation. MCF-7 cells were dosed with radiolabeled 8-oxodG (300 dpm) in the absence or presence of supplemental 100 nM E₂ for 2 days. After incubation, the medium was removed, and the cells were washed three times with PBS. Cells were removed from the plate with trypsin, washed by centrifugation in PBS, and lysed with 1 ml of lysis

solution from the DNA extractor WB kit (Wako Pure Chemical Industries, Richmond, VA). The resulting extracts were filtered by using an Ultrafree-MC centrifugal filter (Millipore, Billerica, MA). The filtered cell extract (100 μ l) was analyzed by HPLC with the same conditions as in the literature (8), briefly with a TSK-GEL DEAE-2SW column and an isocratic elution (75 mM PBS, pH 7.0/20% acetonitrile/1 mM EDTA) at a flow rate of 1 ml/min. All of the authentic standards were purchased from Trilink BioTechnologies, Inc. (San Diego, CA), except for 8-oxodGMP, which was synthesized according to the literature (34). The elution times of the authentic standards of 8-oxodG, 8-oxodGMP, 8-oxodGDP, and 8-oxodGTP were measured with UV detection both at 260 nm and 293 nm run under identical conditions. An alternate HPLC-AMS experiment with a reverse-phase column was performed to confirm the existence of 8-oxodG, 8-oxodGMP, 8-oxodGDP, and 8-oxodGTP in cells (data not shown).

We acknowledge Kurt Hack for preparation of AMS samples and John Vogel for helpful advice and interpretation of the data. This work was performed at the Research Resource for Biomedical Accelerator Mass Spectrometry, operated at University of California Lawrence Livermore National Laboratory under the auspices of U.S. Department of Energy Contract W-7405-ENG-48 and was supported in part by National Institutes of Health Grants RR13461 (to S.S.H., J.M.M., K.W.T., and P.T.H.) and CA55861 (to R.A.S. and J.M.M.) and by the California Breast Cancer Research Program Grant 9KB-0179, (to S.S.H., H.M.K. and P.T.H.).

1. Barnes DE, Lindahl T (2004) *Annu Rev Genet* 38:445–476.
2. Michaels ML, Miller JH (1992) *J Bacteriol* 174:6321–6325.
3. Sekiguchi M, Tsuzuki T (2002) *Oncogene* 21:8895–8904.
4. Mo JY, Maki H, Sekiguchi M (1992) *Proc Natl Acad Sci USA* 89:11021–11025.
5. Sakumi K, Furuichi M, Tsuzuki T, Kakuma T, Kawabata S, Maki H, Sekiguchi M (1993) *J Biol Chem* 268:23524–23530.
6. Furuichi M, Yoshida MC, Oda H, Tajiri T, Nakabeppu Y, Tsuzuki T, Sekiguchi M (1994) *Genomics* 24:485–490.
7. Kamath-Loeb AS, Hizi A, Kasai H, Loeb LA (1997) *J Biol Chem* 272:5892–5898.
8. Nunoshita T, Ishida R, Sasaki M, Iwai S, Nakabeppu Y, Yamamoto K (2004) *Nucleic Acids Res* 32:5339–5348.
9. Hah SS, Kim HM, Sumbad RA, Henderson PT (2005) *Bioorg Med Chem Lett* 15:3627–3631.
10. Neeley WL, Essigmann JM (2006) *Chem Res Toxicol* 19:491–505.
11. Tretyakova NY, Wishnok JS, Tannenbaum SR (2000) *Chem Res Toxicol* 13:658–664.
12. Burrows CJ, Muller JG (1998) *Chem Rev* 98:1109–1151.
13. Cadet J, Douki T, Gasparutto D, Ravanat JL (2003) *Mutat Res* 531:5–23.
14. Henderson PT, Delaney JC, Gu F, Tannenbaum SR, Essigmann JM (2002) *Biochemistry* 41:914–921.
15. Henderson PT, Delaney JC, Muller JG, Neeley WL, Tannenbaum SR, Burrows CJ, Essigmann JM (2003) *Biochemistry* 42:9257–9262.
16. Henderson PT, Neeley WL, Delaney JC, Gu F, Niles JC, Hah SS, Tannenbaum SR, Essigmann JM (2005) *Chem Res Toxicol* 18:12–18.
17. Hailer MK, Slade PG, Martin BD, Sugden KD (2005) *Chem Res Toxicol* 18:1378–1383.
18. Liepold MD, Muller JG, Burrows CJ, David SS (2000) *Biochemistry* 39:14984–14992.
19. Liepold MD, Workman H, Muller JG, Burrows CJ, David SS (2003) *Biochemistry* 42:11373–11381.
20. Hailer MK, Slade PG, Martin BD, Rosenquist TA, Sugden KD (2005) *DNA Repair (Amst)* 4:41–50.
21. Vogel JS (2005) *BioTechniques* 38:13–17.
22. Lappin G, Garner RC (2004) *Anal Bioanal Chem* 378:356–364.
23. Gedik CM, Collins A, European Standards Committee on Oxidative DNA Damage (ESCODD) (2005) *FASEB J* 19:82–84.
24. Collins AR, Cadet J, Moeller L, Poulsen HE, Vina J (2004) *Arch Biochem Biophys* 423:57–65.
25. Russo MT, Blasi MF, Chiera F, Fortini P, Degan P, Macpherson P, Furuichi M, Nakabeppu Y, Karran P, Aquilina G, et al. (2004) *Mol Cell Biol* 24:465–474.
26. Colussi C, Parlanti E, Degan P, Aquilina G, Barnes DE, Macpherson P, Karran P, Crescenzi M, Dogliotti E, Bignami M (2002) *Curr Biol* 12:912–918.
27. Schwarz VA, Hornung R, Fedier A, Fehr MK, Walt H, Haller U, Fink D (2002) *Br J Cancer* 86:1130–1135.
28. Lin X, Ramamurthi K, Mishima M, Kondo A, Christen RD, Howell SB (2001) *Cancer Res* 61:1508–1516.
29. Picard SF, Franco N, Sergent C, Chauffert B, Lizard-Nacol S (2002) *Oncol Rep* 9:971–976.
30. Dingley KH, Ubick EA, Vogel JS, Haack KW (2005) *Methods Mol Biol* 291:21–27.
31. Tsuchiya Y, Nakajima M, Yokoi T (2005) *Cancer Lett* 227:115–124.
32. Li K-M, Todorovic R, Devanesan P, Higginbotham S, Koefeler H, Ramanathan R, Gross ML, Rogan EG, Cavalieri EL (2004) *Carcinogenesis* 25:289–297.
33. Xia Z, Azurmendi HF, Mildvan AS (2005) *Biochemistry* 44:15334–15344.
34. Meyer F, Fiala E, Westendorf J (2000) *Toxicology* 146:83–92.
35. Haghdoost S, Sjolander L, Czene S, Harms-Ringdahl M (2006) *Free Radic Biol Med* 41:620–626.
36. Kennedy CH, Cueto R, Belinsky SA, Lechner JF, Pryor WA (1998) *FEBS Lett* 429:17–20.
37. Kennedy CH, Pass HI, Mitchell JB (2003) *Free Radic Biol Med* 34:1447–1457.
38. Koketsu S, Watanabe T, Nagawa H (2004) *Hepatogastroenterology* 51:638–642.
39. Okamoto K, Toyokuni S, Kim WJ, Ogawa O, Kakehi Y, Arai S, Hiai H, Yoshida O (1996) *Int J Cancer* 65:437–441.
40. Miller H, Prasad R, Wilson SH, Johnson F, Grollman AP (2000) *Biochemistry* 39:1029–1033.
41. Shimizu M, Gruz P, Kamiya H, Kim SR, Pisani FM, Masutani C, Kanke Y, Harashima H, Hanaoka F, Nohmi T (2003) *EMBO Rep* 4:269–273.
42. Nohmi T, Kim SR, Yamada M (2005) *Mutat Res* 591:60–73.
43. Satou K, Kawai K, Kasai H, Harashima H, Kamiya H (2007) *Free Radic Biol Med* 42:1552–1560.
44. Mathews CK (2006) *FASEB J* 20:1300–1314.
45. Kino K, Sugiyama H (2001) *Chem Biol* 8:369–378.
46. Boiteux S, O'Connor TR, Lederer F, Gouyette A, Laval J (1990) *J Biol Chem* 265:3916–3922.